A Vacation-Based Performance Analysis of an Energy-Efficient Motorway Vehicular Communication System

Wanod Kumar, Samya Bhattacharya, *Member, IEEE*, Bilal R. Qazi, *Member, IEEE*, and Jaafar M. H. Elmirghani, *Senior Member, IEEE*

***Abstract*—Due to the unprecedented growth in bandwidth requirement, the increasing number of access points (APs) deployed within a macrocell for services such as video conferencing, video gaming, and data off-loading leads to significantly higher energy consumption. This advancement in mobile networks has forced researchers to explore various methods of energy saving, although with little emphasis on motorway vehicular networks where mobility is also an important aspect. Energy saving in these networks is extremely challenging due to the dynamic nature of the environment in which they operate. To analyze such a network, we first develop a performance model for a medium access control (MAC) protocol, namely, the modified version of packet reservation multiple access (M-PRMA) with wireless channel impairments in a motorway vehicular environment. The M-PRMA protocol provides communication links (time slots) between an AP and the vehicles in range. The time slots of the M-PRMA protocol are modeled as servers where each outage of the channel is represented as a server on queue-length-independent vacation. Then, each AP, in a hierarchical micro–macro topology, is modeled as a single-server queue where the AP takes queue-length-dependent vacations (switches to sleep mode) to save energy during its inactivity period, although at the expense of degraded quality of service (QoS). To address this, a number of sleep strategies for the AP are studied. Finally, both of these proposed models (M-PRMA with channel impairments and AP with sleep cycles) are analyzed and verified through simulations. The performance results reveal that the introduction of sleep strategies at an AP can save up to 80% transmission energy during off-peak hours and 66% on average during the day in a motorway vehicular environment while supporting end-to-end QoS for video and audio conferencing applications.**

***Index Terms*—Channel impairments, energy savings, matrix geometric method (MGM), medium access control (MAC), queueing, sleep, vacations.**

Manuscript received October 2, 2012; revised September 15, 2013; accepted October 2, 2013. Date of publication November 6, 2013; date of current version May 8, 2014. This work was supported by the Engineering and Physical Sciences Research Council through the Intelligent Energy Aware Networks (INTERNET) Project under Contract EP/H040536/1. The review of this paper was coordinated by Prof. J. Deng.

W. Kumar is with the Department of Electronic Engineering, Mehran University of Engineering and Technology, Jamshoro 76062, Pakistan (e-mail: wanod.kumar@faculty.muet.edu.pk).

S. Bhattacharya and B. R. Qazi are with the School of Electronic and Electrical Engineering, University of Leeds, Leeds LS2 9JT, U.K. (e-mail: s.bhattacharya@leeds.ac.uk; b.r.qazi@leeds.ac.uk).

J. M. H. Elmirghani is with the School of Electronic and Electrical Engineering, University of Leeds, Leeds LS2 9JT, U.K., and also with the Department of Electrical and Computer Engineering, King Abdulaziz University, Jeddah, Saudi Arabia (e-mail: j.m.h.elmirghani@leeds.ac.uk).

Color versions of one or more of the figures in this paper are available online at http://ieeexplore.ieee.org.

Digital Object Identifier 10.1109/TVT.2013.2289889

I. Introduction

SINCE the early 1970s, the average distance traveled per year in the U.K. has increased by 53%, resulting in considerably higher average trip length (i.e., 7.1 mi) per person in a day [1]. With the emerging trends of "connected vehicles" in the market, the sheer size of motorway and urban road (transportation) networks with respect to both dimension and users (34.7 million vehicles in the U.K. in 2012 [2]) and the envisaged applications for vehicular communication networks suggest a foreseeable growth that can be parallel with if not higher than that of the current cellular networks. Therefore, it is evident that some of the already existing operational challenges of cellular topology will be inherited in vehicular networks with the added complication of maintaining seamless connectivity in high vehicle mobility. On one hand, a looming spectrum shortage that will strain the support of existing exponential increase in bandwidth requirements rules out the use of incumbent cellular networks to support vehicular communications. On the other hand, extensive base station (BS) deployment to support ubiquitous vehicular network coverage is rendered impractical due to the difficulty of providing high data rates at lower overall costs while maintaining the QoS [3]. Furthermore, the growth of vehicular communication networks comes at a critical point of time where existing communication technologies are already consuming significant amounts of energy, and environmental concerns are increasingly gaining importance [4].

Convergence of energy efficiency paradigms, along with the need for vehicular applications, forces us to take account of the power-hungry nature of BS entities in cellular networks and to minimize energy use in vehicular communication networks through a heterogeneous use of microcells/picocells served by APs within a macrocell that enable higher data rates [3]. Furthermore, these APs serving small cells can utilize sleep strategies dependent upon traffic intensity [5]. Such strategies are impractical for BS-only scenarios due to the larger resource activation time and high overhead that may arise from the ping-pong effect of consistently turning a BS on and off [6]. Energy efficiency and sleep strategies in vehicular networks are further discussed in Section II. An AP performs somewhat similar operations to that of a BS, although at a much smaller scale, making it feasible for it to switch into a low-power state and then back to the fully operational state in relatively small time. This results in a remarkably low overhead compared with that of a BS. Therefore, it is worthwhile studying whether an

effective sleep strategy can be applied to the APs to save energy. The introduction of sleep strategies for an AP redefines the performance (analysis) from both QoS and energy perspectives.

In a motorway vehicular network, provisioning real-time services while maintaining the respective QoS is quite challenging due to the dynamic nature of vehicles and the variable wireless channel conditions [7]. This problem becomes more severe due to the high relative speed difference between fast-moving vehicles and a stationary AP/roadside unit (RSU) in a motorway environment. Unlike carrier-sense multiple access (CSMA), deterministic protocols such as time-division multiple access (TDMA) are best suited to supporting centralized communications as these protocols define a certain upper bound on the channel access delay even if the channel is heavily loaded [8]. CSMA-based protocols severely suffer due to collisions or collision avoidance overhead, particularly in high load conditions, making it unsuitable for a motorway vehicle-to-roadside (V2R) environment; this has also been reiterated in [9]–[11]. Therefore, we utilize a TDMA-based protocol, namely, the modified version of the packet reservation multiple-access (M-PRMA) protocol, in this paper. The M-PRMA was introduced in [12] for communications between vehicles and the AP; however, its performance with realistic channel characteristics has not been studied so far.

To the best of our knowledge, detailed analytical and simulation models of a V2R motorway network that maintains end-to-end QoS while incorporating real wireless channel impairments at the M-PRMA protocol and introducing sleep strategies at APs to save energy have not been developed so far. Thus, our contribution in this paper is fourfold.

1) We develop an analytical queuing model of the aforementioned V2R communication scenario using a matrix geometric method (MGM) where the M-PRMA protocol with realistic wireless channel characteristics is considered. Since the M-PRMA is a slot-based protocol, we have represented these slots[1] as servers and the outage of a slot as a server on vacation. Thus, the model becomes an $M/M/c/\infty/M$ queuing system with asynchronous queue-length-independent vacations.
2) We validate the proposed analytical model by reducing it to a simple $M/M/c/\infty/M$ model without vacation by setting the number of fades in the channel equal to zero (idealistic channel scenario), and then compare its performance with the existing $M/M/c/\infty/M$ model [13]. We further study the impact of varying level-crossing rate (wireless channel characteristics) on the number of slots (servers in this case) in terms of utilization, average packet delay, and packet-loss ratio. The performance results of the system are verified with simulations with respect to varying vehicular load, where both real vehicular traffic profiles (M4 motorway, U.K. [14]) and data packet measurements [15] are utilized.
3) The departure process of the M-PRMA protocol becomes an arrival process at the AP. The AP with a wireless link to the main BS can be modeled as a single-server queue ($M/M/1/K$) where the AP takes vacations (switches to sleep mode) to save energy during its inactivity periods.
4) To validate the analytical model of the AP, we reduce the proposed $M/M/1/K$ MGM model with vacations to a simple $M/M/1/K$ model without vacations by setting the mean arrival rate from vacation equal to zero, and we compare the performance parameters with an $M/M/1/K$ model. The impact of varying data rates, buffer sizes, and sleep cycles on the system are studied to find optimal values for these parameters. Both proactive and reactive random sleep strategies for the AP are studied. Thereafter, we evaluate the performance of the system in terms of energy savings, average packet delay, and packet-blocking probability.

Following the introduction, this paper is organized as follows. In Section II, the related work is discussed. Section III summarizes the studied scenario. The analytical model and the performance results of the M-PRMA protocol with channel characteristics are detailed in Section IV. The mathematical modeling and performance evaluation of the AP architecture are discussed in Section V. This paper concludes in Section VI.

II. Related Work

Wireless channels in an outdoor environment are unpredictable and thus pose several challenges to system designers. This problem becomes more challenging in vehicular networks, particularly in a motorway environment, as the topology changes quite frequently due to the relative speed difference between fast-moving vehicles and a central coordinating entity (for example an AP). In [7], deterministic propagation models were used to analyze the performance of vehicular systems in the presence of a line-of-sight link; however, their suitability for real channel characterization has been questioned [16]. According to [17], for a low transmit power in microcells, a wireless link could be established for a 0.2–1 km (microcellular communications) range between a vehicle and an RSU or a BS. In a motorway vehicular microcellular network, the received signal envelope follows a Rician distribution, and a multiray tracing technique can be employed to predict the received signal [17]. As the topology changes very quickly and frequently in these networks, a ray-tracing-based technique may not be suitable, although some researchers have employed this method in their work [18]. Field measurements provide a useful insight into the characterization of a wireless channel for the vehicular environment [19]–[21]. Path-loss exponent v, shadowing standard deviation σ_d, and break point distance d_b are considered the main parameters when modeling wave propagation. In [21], field measurements were conducted at 871.26 MHz for macrocellular systems for urban, suburb, and highway scenarios. It was found that, in the highway scenario, the path-loss exponent and standard deviation are approximately 4.28 and 2.79 dB, respectively. In [20], the measurement setup at 1700 MHz for a highway microcellular system, i.e., $v = 3.37$ and $\sigma_d = 0.46$ dB, were determined with the help of curve fitting applied to the practical data. Thus, the path loss can be adequately described by an inverse power law value of 3.4. When a double-regression analysis was applied for the same

[1]Note that, in this paper, slots, servers, and links are used interchangeably.

measurements, inverse square law was consistently observed for the first slope, but the gradient of the second slope was found to be an increasing function of the break point distance.

The medium access control (MAC) protocols in a motorway vehicular environment are of significant importance [22] as they need to handle several issues such as smooth interaction with other communication layers, time synchronization, rapid channel variations due to the fast movement of vehicles, and handoff problems in the centralized networks [12]. TDMA-based protocols have traditionally been preferred over CSMA-based protocols in a motorway V2R environment as the latter performs poorly at high load [8]–[11]. In [24], a collaborative MAC protocol called vehicle-and-roadside collaborative MAC protocol has been proposed for a highway scenario that utilizes TDMA for centralized communications and CSMA for intervehicular communications. This study was carried out only through simulations without considering real channel impairments and analytical modeling. This work was further extended in [24] by incorporating physical-layer impairments in terms of shadowing. However, only simulations were carried out to evaluate the performance of the system. To enable data communications in a vehicle-to-vehicle network, an adaptive distributed cooperative MAC protocol called ADC-MAC has been proposed in [25]. The performance of this protocol was analyzed using Markov-chain-based modeling, and simulations were carried out in Network Simulator ns-2. This protocol leveraged cooperative communications based on spatial and user diversities; however, such a protocol is infeasible in a motorway V2R network. In [26], Chen *et al.* described a multiserver multipriority queueing model for vehicular access networks using $M/M/c$ and $M/G/c$ queues. Since the number of communicating nodes was finite in [26], queues with finite population could have been more appropriate models. In [12], another TDMA-based protocol was introduced and modeled as an $M/M/c/\infty/M$ queue for a motorway vehicular environment, namely, M-PRMA protocol. The performance of the M-PRMA protocol was evaluated in terms of *throughput*, *delay,* and *packet-dropping probability*, although in idealistic channel conditions (without any physical channel impairments). The performance evaluation and comparison of the M-PRMA protocol with the IEEE 802.11p MAC protocol in a motorway vehicular environment (without any analytical modeling and physical channel impairments) showed that CSMA/collision avoidance (CSMA/CA)-based IEEE 802.11p protocol scaled poorly at high load in terms of QoS (average access delay, packet-loss ratio, and goodput) and energy consumption [11]. For instance, as vehicles constantly listened to the medium for collision avoidance under 802.11p, they achieved only 50% goodput and consumed 12 times higher energy compared with that under M-PRMA protocol [11], which is our preferred choice for a motorway V2R network in this paper. In [27], an $M/M/c$ queue was analyzed with queue-length-independent vacations of the servers, and their impacts on the average system delay and system utilization were studied. However, adopting such an analysis in the context of dynamic motorway V2R environment merits extension in terms of various vehicular communication parameters such as fade duration, level-crossing rate, and packet-loss ratio. All these parameters have been described later in the paper. To the best of our knowledge, queueing and simulation models of the M-PRMA protocol with physical channel impairments where channel outage is modeled as a server on queue-length-independent vacation have not been developed and analyzed so far while considering real packet measurements and real vehicular traffic profiles.

The power consumption of a node for transmission is divided into two parts (i.e., power consumed in electronic circuitry and power consumed by an output amplifier). In the case of signal reception by a node, the total power consumption is due to the receiver's electronic circuitry only. The results reveal that power savings can be achieved during the transmission activity by optimizing the transmit power levels at the source nodes. In [28], RF output power optimization strategy was utilized to achieve energy savings, and the results showed that a significant amount of power could be saved with multihop communications, as compared with direct communications from a source to the BS. Instead of RF output power optimization strategies, a different view was presented in [29] where circuitry was shown to consume very high power compared with the output amplifier power while transmitting. Other studies showed that, by considering a sleep strategy at a node during its inactivity, a certain amount of energy could be saved [30], [31]. The phenomenon of switching off the transmitting circuitry and thus setting the transceiver into a low energy state is called sleep [32]. Recent sleep strategies have been an attractive solution to reducing network energy consumption as it does not need a complete overhaul of network devices and protocols. In [33] and [34], a sleep strategy for the line cards in the routers depending upon the backbone traffic was proposed. Their heuristic achieved 79% reduction in energy consumption, which was accounted for the low link utilization (30%) in the Internet service providers (ISPs) backbone. Such major reduction may not be feasible in wireless and mobile networks (e.g., cellular or vehicular) as they are not intrinsically overprovisioned and the link quality being dependent upon the varying wireless channel makes it susceptible to degraded QoS. Nevertheless, several research groups around the world are considering various sleep strategies to make cellular network energy efficient [3], [35], [36]. In [35], dynamic switching for a BS in low traffic conditions was proposed. However, fast switching may not be feasible to accommodate transient traffic behavior because of the number of operations that a large BS has to perform [6]. This makes the architecture inapplicable for vehicular networks. In another study [36], a periodic sleep strategy for a cellular network was studied, leading to a 46% reduction in operating energy expenditure. However, the architecture proposed was of multilayered type and deployed a cell breathing technique. Again, the cell breathing solution with its incurred overhead cannot accommodate fast user movement and variation in traffic demand, making it inapplicable for vehicular networks, particularly in a motorway environment. One of the solutions to this problem is to use a macro–micro (hierarchical) cell structure [3], which decreases the overall energy consumption (area power consumption) of a network. In this type of architecture (considered in this paper), the main BS is also responsible for signaling and coordination of a number of microcells, which are powered by APs/RSUs, under its coverage [5]. Since the APs have low switching

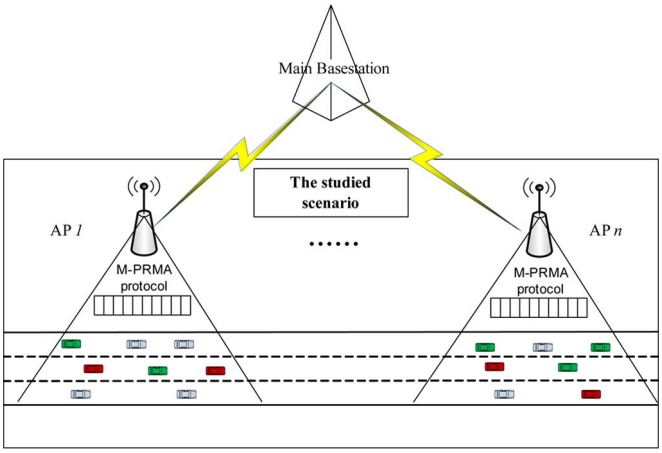

Fig. 1. Studied scenario.

overhead, they can periodically sleep and wake up very fast to accommodate transiency in user demand. The wake-up overhead of an AP is discussed in detail later in the paper. In [37], the IEEE 802.11 Power Save Mechanism was enhanced to achieve energy savings in vehicular networks, although without any sleep mechanism. Further, the only QoS parameter considered in their work, with respect to energy savings, was end-to-end delay. Thus, the other key QoS parameter for real-time communications, i.e., the *packet-blocking probability*, was not considered. In [27], an $M/M/c$ queue was analyzed with queue-length-dependent vacations of the servers, and their impacts on the average system delay and system utilization were studied. However, to the best of our knowledge, queues with vacations have not been utilized in the context of energy savings so far.

III. Studied Scenario

The studied scenario is based on a typical centralized motorway vehicular communication system, as shown in Fig. 1, where communications between vehicles and an AP is enabled through a wireless link using the M-PRMA protocol [12]. The objective is to evaluate the performance of the given system from energy and QoS perspectives. The studied architecture resembles the hierarchical macro–micro cellular topology whose advantages have been identified in [3]. Each AP in the studied scenario provides coverage of 1 km (in line with the Wireless Access in Vehicular Environments standard [38]), where eight APs are connected to a main BS. The number of APs connected to the BS depends upon the standard data rate specifications of the APs and the BS. Thus, it is reasonable to consider a stretch of 8 km to analyze the network. The time slots of the M-PRMA protocol (wireless links) can be modeled as a multiserver queue. Further, since the wireless channel is unpredictable in a dynamic vehicular environment, the unavailability of the links needs to be incorporated in the model. Therefore, we determine the number of fades per second (level-crossing rate) and average fade duration, which depend upon several parameters such as vehicle speed, operating frequency, fading statistics, receiver sensitivity, and average received power [39]. The channel outage can be obtained from the given scenario, which is modeled as a server (slot) on *queue-length-independent asynchronous vacation*.

The served packets from the M-PRMA protocol arrive at the input buffer of the APs and are subsequently transmitted to the main BS where an AP can be represented as a single-server finite buffer queue. In this scenario, the AP operates sleep cycles to save a significant amount of energy during its inactivity period. Hence, the AP with sleep cycles is modeled as a single-server finite buffer queue, where the server takes *queue-length-dependent vacation*. We solve these two queues in tandem to ensure the QoS while saving a significant amount of energy. In this paper, since we consider audio and video conferencing models [40], symmetric traffic is therefore assumed. Hence, the performance of uplink (vehicles to the AP) transmission is evaluated without loss of generality.

IV. Modified Version of Packet Reservation Multiple Access Protocol With Realistic Channel Characteristics

Since the M-PRMA protocol with idealistic channel characteristics was modeled as an $M/M/c/\infty/M$ queue in [12], we extend here the model to incorporate real channel characteristics.

A. Mathematical Modeling

In a communication scenario with the M-PRMA protocol, a packet generated by a vehicle waits for an available slot for transmission. The packet is only dropped if the channel becomes bad during its transmission. The outage of the channel is modeled as a two-state Markov chain, where the transition rates are obtained from the level-crossing rate (i.e., in fades per second) and average fade duration t_{out}. In [27], asynchronous queue-length-independent vacations for an $M/M/c$ queue were introduced. In this paper, we extend the vacation model in [27] to incorporate the channel outage as a server on vacation. Note that the assumption of an infinite buffer is to represent the packet transmission policies of the M-PRMA protocol, where packet loss occurs only due to channel impairments. Here, the time slots in M-PRMA [12] are considered c independent servers, and the vacations are asynchronous, i.e., independent of queue length, representing channel outage. Let the arrival process of the packets from each of the M vehicles be Poisson distributed with mean rate λ'. Thus, for a packet-switched network, where a vehicle becomes idle until the arrival of the next packet (after transmitting the packet), the combined arrival process can be represented as a Poisson distribution with mean $\lambda = M\lambda'$. Further, the service time for each packet is assumed to follow a negative exponential distribution with mean $t = (1/\mu)$, where μ is the mean service rate of each server. Evidently, a packet can be only served if a server is available (not on vacation). The vacation time is assumed to be negative exponentially distributed with mean $t_{\text{out}} = (1/\delta)$. Hence, the arrival rate of servers from vacation is $j\delta$, where $0 \leq j \leq c$. The availability time of a server is negative exponentially distributed with mean $t_{\text{av}} = (1/\gamma)$. Thus, the server departure rate due to outage is $j\gamma$, where $0 \leq j \leq c$. The state diagram of this scenario is shown in Fig. 2 with a lexicographical representation. Each state is represented by pair (j, k), where $j = 0, 1, 2, \ldots, c$ represents the number of available servers, and $k = 0, 1, 2, \ldots, \infty$ represents the number of packets in the system.

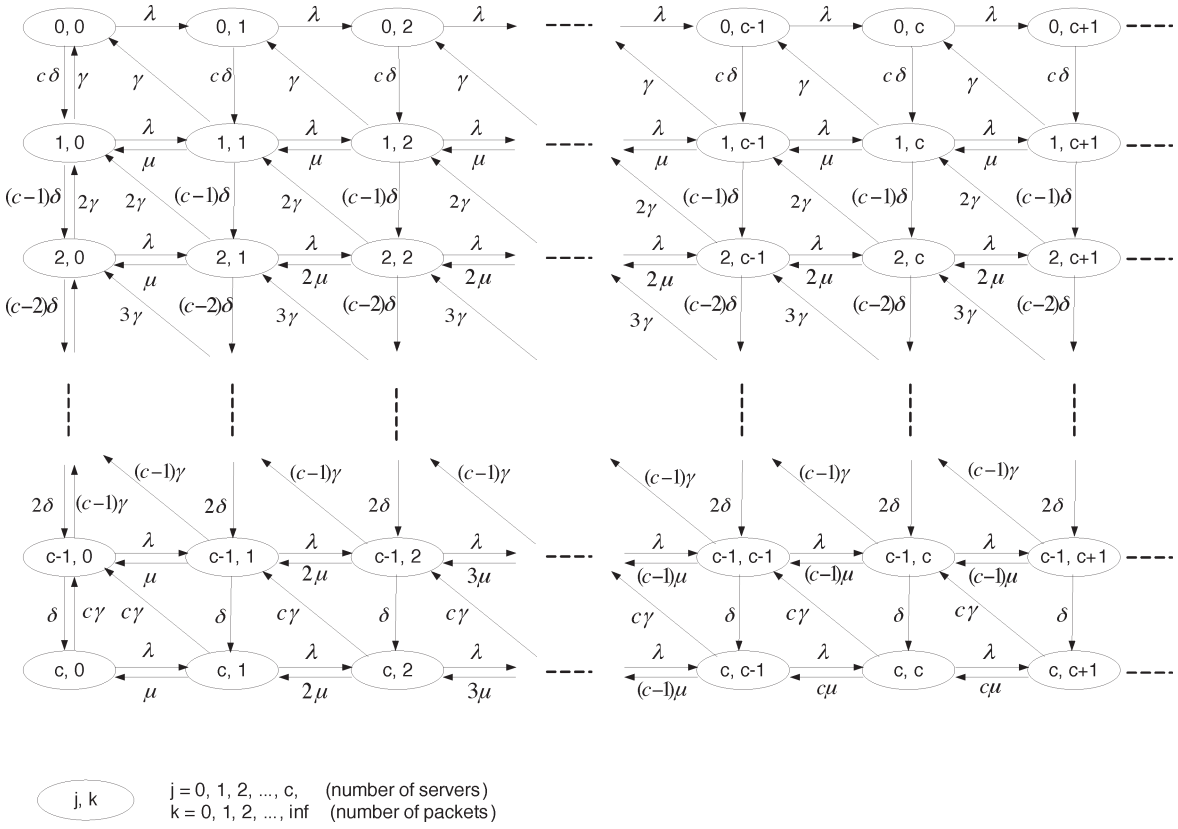

Fig. 2. State transition diagram of M-PRMA with vacation.

TABLE I
SYSTEM PARAMETERS

Variable	Notation	M-PRMA	AP
Up-link channel data rate	d_r	12 Mbps [42]	27 Mbps [42]
No of slots/servers	c	12	1
Video conferencing data rate per node	d_t	320 kbps [41]	N/A
Average packet size	P_S	867.4 Bytes [15]	867.4 Bytes [15]
Packet arrival rate	λ	$d_t/(P_S \times 8)$	N/A
Packet service rate per slot	μ	$d_r/(P_S \times 8)$	$d_r/(P_S \times 8)$
Max. operational power	P_{MAX}	N/A	30 W[42]
Min. operational power	P_{MIN}	N/A	$P_{MAX}/1.3548$ [33]
Transmit power	P_t	N/A	$P_{MAX} - P_{MIN}$ [33]
Energy for wake-up overhead	E_{wo}	N/A	0.0175 J

A detailed mathematical modeling is presented in Appendix A. From (24), the mean queue length N can be computed as

$$N = \sum_{k=0}^{\infty} k p_k. \tag{1}$$

The average packet delay W can be obtained using *Little's theorem* as follows:

$$W = \frac{N}{\lambda}. \tag{2}$$

System utilization U, which is the probability that the servers are busy, can be defined as

$$U = \frac{\sum_{j=1}^{c} \sum_{k=1}^{\infty} \min(j,k) p_{jk}}{c} \tag{3}$$

where p_{jk} is the probability of k packets when there are j available servers.

To determine the packet-loss ratio due to channel outage, we compute the difference of the utilization of the systems with and without loss. Note that, in the lossless system, if a server becomes unavailable due to a vacation, the packet waits for the next available server and hence is not dropped. The system parameters are given in Table I. In this paper, an uplink channel frame of the M-PRMA protocol is subdivided into 12 slots, each operating at 1 Mb/s.

In Section V, notations P_t and E_{wo} denote the transmitter power of the AP and the energy wake-up overhead, respectively, as shown in Table I. The energy model utilized in this paper is based on [11], where energy per bit (in the transmission state) can be determined, if required, as a ratio between the transmitter power and the data rate [11]. Energy savings are achieved at the AP through sleep mode, where the transmitter part of the AP is switched off. The ratio between the fully operational power and the low state power is based on [32]. We have assumed a reference value of 0.0175 J for a sleep cycle (energy) overhead

TABLE II
NUMBER OF SLEEP CYCLES N_S

Hours	Vehicular density [14]	Bounded delay	Bounded blocking	Random sleep cycle (10 ms)
0000-0059	3	265746	26564	349470
0100-0159	3	264716	26455	347940
0200-0259	2	266547	17261	348570
0300-0359	2	267925	17236	351960
0400-0459	2	267059	17190	348480
0500-0559	4	264114	36060	342290
0600-0659	10	247166	94538	318820
0700-0759	24	202703	188687	261220
0800-0859	31	187395	210839	232430
0900-0959	23	203999	183863	268450
1000-1059	20	213764	169074	279400
1100-1159	20	214030	169457	280540
1200-1259	23	203966	183919	262840
1300-1359	26	196785	196282	254350
1400-1459	30	191580	208352	239060
1500-1559	32	196200	213305	228870
1600-1659	34	218750	216006	223060
1700-1759	35	236468	217687	215130
1800-1859	30	190940	208197	237000
1900-1959	27	193063	199581	246510
2000-2059	17	223132	151418	290800
2100-2159	11	242085	103226	314940
2200-2259	9	247632	85025	322590
2300-2359	5	261651	45942	337440

in (8); however, a more fundamental overhead parameter, namely, sleep count (the number of times the AP has to wake up), is also calculated for both proactive and reactive sleep strategies. The respective sleep counts are presented in Table II.

B. Simulation Process for M-PRMA With Realistic Channel Characteristics

To implement the M-PRMA protocol with realistic channel condition, we have extended the JAVA-based event-driven simulator introduced in [12] where key vehicular traffic and mobility characteristics were implemented based on a detailed statistical analysis on experimental vehicular measurements obtained from the M4 motorway, U.K. The simulator is comprised of four classes: 1) a *vehicle* class that maintains vehicular mobility; 2) a *slot* class that keeps track of the unavailability of a slot due to service and/or channel outage; 3) a *distribution* class that is used to generate the packet arrival, packet size, and slot outage duration; and 4) the *main* class to run the simulation. All c slots are scanned at each time instance. If a packet arrives, it is either served by one of the available slots or waits until it obtains a slot. The corresponding actions are associated to service time or waiting time, respectively, which in turn are used to calculate the average packet delay. Upon the arrival of a slot vacation, the slot is made unavailable for exponentially distributed time, and the packets being served or arriving during this period are lost, which accounts for the packet-loss ratio. The successfully transferred packets form the arrival process at the AP. The simulation is run in microseconds for a period of 3600 s, representing an hour, to calculate the QoS parameters based on variables incremented and packet timestamps used during that hour. The hour is then incremented, and the simulator updates the vehicular density to get the results for each hour of the day.

C. Results

Considering a 2.4-GHz frequency band, we assume an AP antenna height h_a of 10 m with a 3-dBi gain and vehicle antenna height h_v of 1.5 m with a 0-dBi gain [11]. A vehicle, moving at an average speed of 30 m/s on a typical motorway [12], transmits data with average transmit power P_t of 30 dBm. According to [41], a power threshold $P_{\rm th}$ of -90 dBm is required at the receiver to support communications with channel capacity d_r of 12 Mb/s. With the aforementioned parameters, the mean received power P_r at a distance of 500 m (assuming that the AP is at the middle of 1-km stretch) becomes -70.8 dBm. Using these parameters, we compute the level-crossing rate $c\gamma$ and average fade/outage duration $t_{\rm out}$ in the channel [39], which result in 65.255 fades/s and 0.183 ms, respectively. Since, in the M-PRMA protocol, the channel is divided into a number of slots, therefore, the number of fades per slot γ can be also determined. Furthermore, a flat fading channel has been considered, and if a channel slot is unavailable due to outage, then the packet becomes erroneous and thus considered lost.

Here, we first validate the proposed analytical model with an $M/M/c/\infty/M$ model (without vacations) by considering the maximum number of vehicles (i.e., 35) recorded from the M4 motorway data [14]. Then, we study the effect of the level-crossing rate (number of fades per second) on a varying number of servers (data rate) in terms of QoS parameters. Thereafter, we evaluate the performance of the system in terms of utilization, average packet delay, and packet-loss ratio with varying vehicular load over 24 h. It should be noted that we consider real-time data communications where each vehicle generates data traffic at 320 kb/s and the packet size distribution is random with a mean of 867.4 B [15]. Where applicable, the analytical results are verified with simulations, and both are found to be in good agreement.

1) Analytical Model Verification: To validate the analytical model, we reduce the proposed $M/M/c/\infty/M$ model with vacations to a simple $M/M/c/\infty/M$ model without vacation by setting the level-crossing rate (number of fades in the channel) equal to zero, and we compare the performance parameters, namely, utilization and average packet delay, with an $M/M/c$ model. With $M = 35$, a traffic generation rate of 320 kb/s/vehicle, average packet length of 867.4 B, and uplink channel of 12 Mb/s, the minimum number of servers c should be 12 (each operating at 1 Mb/s) to ensure system stability ($\lambda/c\mu < 1$). With 12 servers (time slots of the M-PRMA) in the system, the utilization for both models is found to be 93%. However, it decreases with an increase in the number of servers due to the higher effective channel data rate, which is expected. With 36 servers in the system, the utilization for both models is 31%. Similarly, the average packet delay steeply decreases with an increase in the number of servers because of the effective increase in the service capacity. Each packet suffers an average delay of 13.4 ms with 12 servers in the system because of high utilization. However, it reduces and stabilizes as the effective number of servers increases. With $c \geq 21$, the average delay experienced by the packets is only due to the service in the server. Note that the service time depends upon the capacity of each server and is independent of the number of servers.

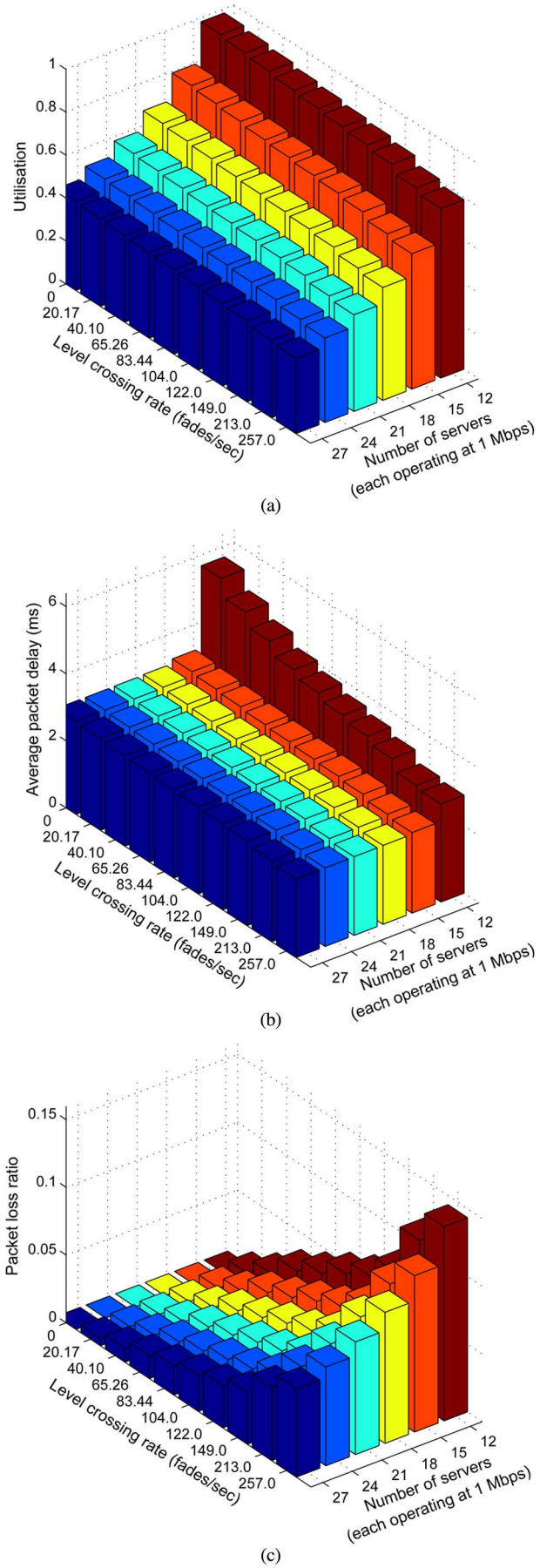

Fig. 3. Varying level-crossing rate and number of servers. (a) Utilization. (b) Average packet delay. (c) Packet-loss ratio.

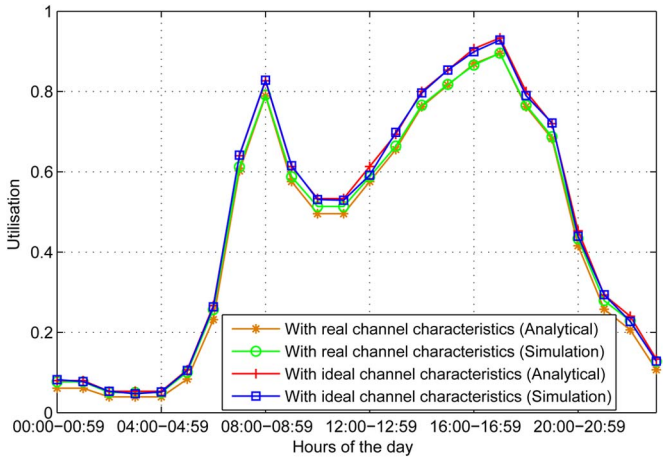

Fig. 4. Utilization with varying vehicular load.

2) Impact of Varying Level-Crossing Rate on Utilization, Average Packet Delay, and Packet-Loss Ratio: As previously mentioned, the level-crossing rate (number of fades per second), which defines the behavior of a wireless communication link, is dependent upon several parameters such as the vehicle speed, operating frequency, fading statistics, receiver sensitivity, average received power, etc. [39].

As anticipated, the utilization in Fig. 3(a) decreases with an increase in the number of servers because the servers increase the overall capacity of the system. Moreover, a steep decrease in utilization with an increase in the level-crossing rate is noticed due to the impact of packet loss [see Fig. 3(c)]. Since the average packet delay in Fig. 3(b) is only estimated for the successfully served packets, therefore, it decreases with an increasing level-crossing rate. With a level-crossing rate of zero representing an ideal channel, the packet-loss ratio [see Fig. 3(c)] is also zero for all servers (data rates). With an increase in the level-crossing rate, the packet-loss ratio also increases as channels become more prone to errors. The impact of a higher level-crossing rate is more severe on the lower number of servers as fades per second are distributed among the number of servers. Hence, a higher number of servers increases reliability and decreases the packet-loss ratio at the cost of lower utilization.

3) Performance Evaluation: Here, we evaluate the performance of the proposed model with $c = 12$, level-crossing rate of 5.44 fades/s/server, and varying vehicular density that corresponds to the hours of the day.

a) Utilization: Fig. 4 shows the utilization of the system with varying vehicular load for real and ideal channel conditions. As can be realized from (3), the utilization is dependent upon both the number of available servers and the carried load. Thus, it follows the trend of vehicular density [14] (see Table II). At 17:00, the utilization is 0.9, corresponding to a very high load at the peak hour. However, it is only 0.04 during the off-peak hours. It is evident that the utilization in ideal channel conditions will be higher at any point than that with real channel conditions, which takes the packets dropped due to fading into account.

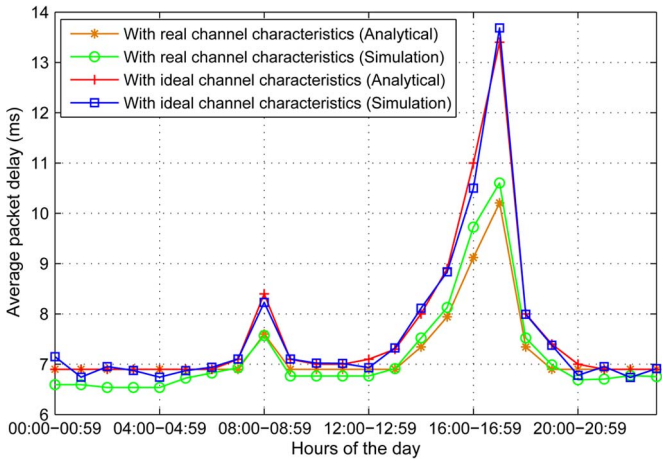

Fig. 5. Average packet delay with varying vehicular load.

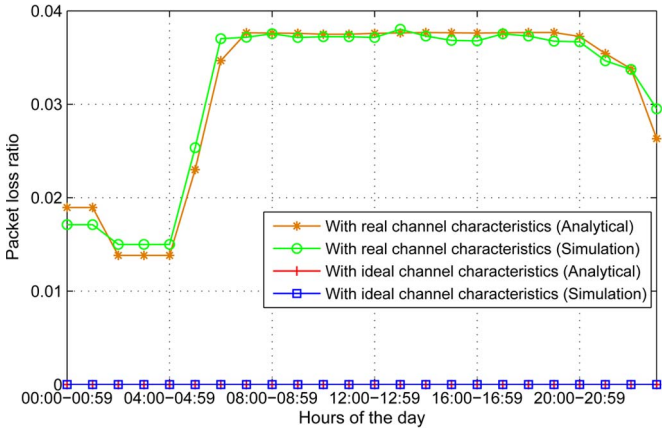

Fig. 6. Packet-loss ratio with varying vehicular load.

b) Average packet delay: Fig. 5 shows the variation of average packet delay for both real and ideal channel conditions. As can be realized from (2) for a fixed number of servers, the average packet delay is dependent upon the mean number of packets (which increases with an increase in traffic load) in the system. Moreover, the average packet delay is higher during the peak hour (17:00) because a packet, on average, has to wait for longer duration before being served. During the off-peak hours, the minimum average packet delay is due to the service time only without any waiting delay. It is to be noted that the scenario with real channel conditions incurs a lower average packet delay than that of the scenario with ideal channel conditions because the dropped packets due to fading do not contribute to the delay.

c) Packet-loss ratio: The packet-loss ratio due to channel outage is shown in Fig. 6. During the off-peak hours, the system experiences a low packet-loss ratio (i.e., ≤ 0.02). Since the slots and their fades are independent of each other, and the number of fades and their duration times are very low/small, therefore, the packet-loss ratio with a lower number of vehicles (representing off-peak hours) is low. The packet-loss ratio is higher ($\backsimeq 0.038$) in the case of average-to-peak hours as the probability of finding a slot in outage becomes higher. Note that, although the utilization becomes high due to higher load (average to maximum number of vehicles), the impact of varying high load on the packet-loss ratio is negligible as it only reflects the channel impairments unlike [12], where a packet used to get dropped when its delay reaches a certain threshold. Likewise, there is no packet loss in the case of ideal channel conditions (in the absence of fading).

V. Access Point Architecture

The departure process of the M-PRMA protocol becomes an arrival process at the AP (which transmits packets to the main BS), where interdeparture time of the packets from the M-PRMA protocol has been analyzed through simulations for 2 vehicles (the minimum number), 20 (the average number), and 35 (the maximum number) of vehicles. The interdeparture time in each case is found to be negative exponential distributed. This is due to the effect of Poisson distributed arrival of packets from the vehicles and random events of channel unavailability at the M-PRMA link. The AP switches to low-power mode (i.e., sleep) if there is no packet in service or waiting to be served. It remains in that state for an exponentially distributed time duration with a preset mean value. The AP wakes up at the end of this time duration and checks if there is any packet to be served. If the buffer is still empty, the AP goes back to sleep mode. Otherwise, it starts serving that packet. This procedure is called sleep cycle. The introduction of sleep cycles (to save energy) at the AP calls for an advanced queueing model, which ensures QoS. We represent this as an $M/M/1/K$ queue with queue-length-dependent vacations.

A. Mathematical Modeling

The departure process of the M-PRMA protocol with channel impairments follows a Poisson process with mean rate λ_s and therefore becomes the arrival process at the AP with the interarrival time following negative exponential distribution. The AP with a finite buffer of size K and a negative exponential service with mean service time $t_s = (1/\mu_s)$ is modeled as an $M/M/1/K$ queuing system with queue-length-dependent vacation [27]. The server in this case is the link between the AP and the main BS with a mean service rate of μ_s. It takes a negative exponentially distributed vacation with mean vacation time $t_v = (1/\delta_v)$ when the system is empty to save energy, where δ_v is the arrival rate of the server from vacation. On arrival from a vacation, if the server finds any packet in the system, then the packet is served immediately; otherwise, the server takes another vacation. In this system, the variable mean availability time of the server is not present because the vacation is queue length dependent. The state diagram of this system is shown in Fig. 7 with a lexicographical representation, where each state is represented by a pair (j, k), where $j = 0, 1$ represents the server on vacation or the available server, and $k = 0, 1, 2, \ldots, K$ is the number of packets in the system. In Fig. 7, state (1, 0) is inseparable with state (0, 0) because the server, although returning from a vacation, takes another vacation if there is no packet in the system.

A detailed mathematical modeling is presented in Appendix B. From (31), the mean queue length or system size N_s can be

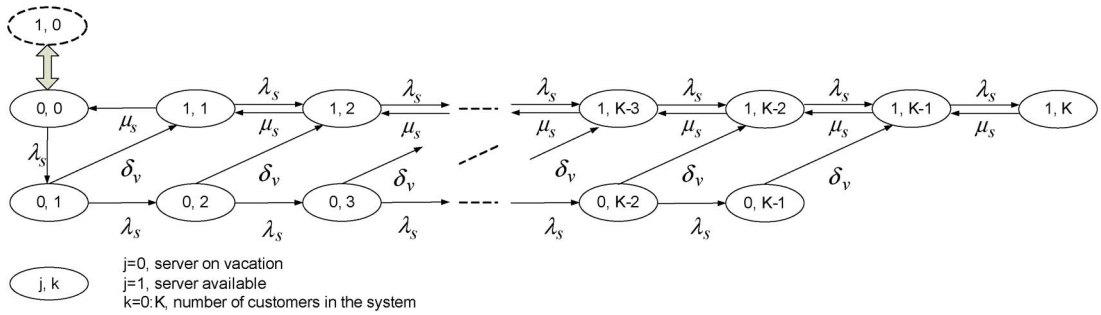

Fig. 7. $M/M/1/K$ system with vacation.

computed as

$$N_s = \sum_{k=0}^{K} k p_k. \tag{4}$$

Packet-blocking probability P_B is the probability that an incoming packet finds the system full. It is the sum of the probabilities of states $(0, K-1)$ and $(1, K)$. Therefore

$$P_B = \pi_{0(K-1)} + \pi_{1K}. \tag{5}$$

The average delay W_s for a packet at the AP can be computed using Little's theorem as follows:

$$W_s = \frac{N_s}{\lambda_s(1 - P_B)}. \tag{6}$$

System utilization U_s is defined as

$$U_s = \frac{\lambda_s}{\mu_s}(1 - P_B). \tag{7}$$

The energy savings at the AP, during its inactivity period, is given by

$$E_s = (1 - U_s) \times P_t \times 3600 - (E_{\text{wo}} \times N_S) \tag{8}$$

where N_S refers to the number of sleep cycles (sleep count).

B. Simulation Process for the AP With Sleep Cycles

We extend the developed JAVA-based simulator [12] to implement sleep cycles at the AP. The main difference between the implementations, which are shown here and in Section IV-B, is the type of vacation. The vacation in M-PRMA, representing channel impairment, is queue-length independent, whereas the vacation in AP, representing a sleep cycle to save energy, is queue-length dependent. In the case of the buffer of the AP being full, the newly arrived packet is blocked, which accounts for the packet-blocking probability. Otherwise, the packet is added to the buffer, and the waiting time is registered. This waiting time is used to calculate the average packet delay. The AP may become unavailable for the first packet waiting in the buffer due to two reasons: it is either serving another packet or is in the low-power state due to a sleep cycle. The AP switches to sleep mode with exponentially distributed time duration with a certain mean if it is not serving any packet and if the buffer is empty. This affects the utilization of the AP and, hence, energy savings, as shown in (8). Counter *sleepCount* is defined to count the number of times the AP has gone to sleep mode. This accounts for the associated energy overhead. Upon waking up, the AP starts serving the packets waiting in the buffer and does not switch to sleep mode until it has served all the waiting packets.

C. Results

Here, we first validate the proposed analytical MGM model without vacations using a traditional $M/M/1/K$ model [13]. Then, the impacts of varying data rate, buffer size, and sleep cycles are studied. Based on these, we introduce three operating strategies (bounded packet-blocking probability, bounded average packet delay, and fixed random sleep) to evaluate the performance of the system in terms of energy savings, average packet delay, and packet-blocking probability with varying M4 vehicular load over 24 h of the day. Where applicable, the analytical results are verified with simulations, and both are found to be in good agreement.

1) Model Verification: Considering a data rate of 12 Mb/s (AP to main BS), the impact of varying load with different buffer sizes (10, 20, and 30) on the system is studied. With an increase in load (i.e., number of arrived packets per unit time), the system becomes more utilized, and the utilization gradually saturates toward its maximum, as shown in Fig. 8(a). Further, an increase in buffer size increases the system utilization in general because the AP has to process a higher number of waiting packets in its buffer. The impact of buffer size on utilization is subtle at lean load due to the insufficient packets in the underutilized system. It is observed in Fig. 8(b) that the system accommodates a certain increase in load without affecting the delay during lean period as the preprocessing times for the packets are negligible. It is evident that a larger buffer size can accommodate more packets, which in turn, incurs additional preprocessing delay at the AP due to the increased number of packets waiting in the queue during peak hours. Unlike the average packet delay, the packet-blocking probability, shown in Fig. 8(c), decreases with an increase in the buffer size because it can accommodate more packets, which otherwise would have been blocked due to buffer overflow. Thus, a suitable choice of buffer size is crucial in system design to maintain both the average packet delay and the packet-blocking probability under their respective operating thresholds.

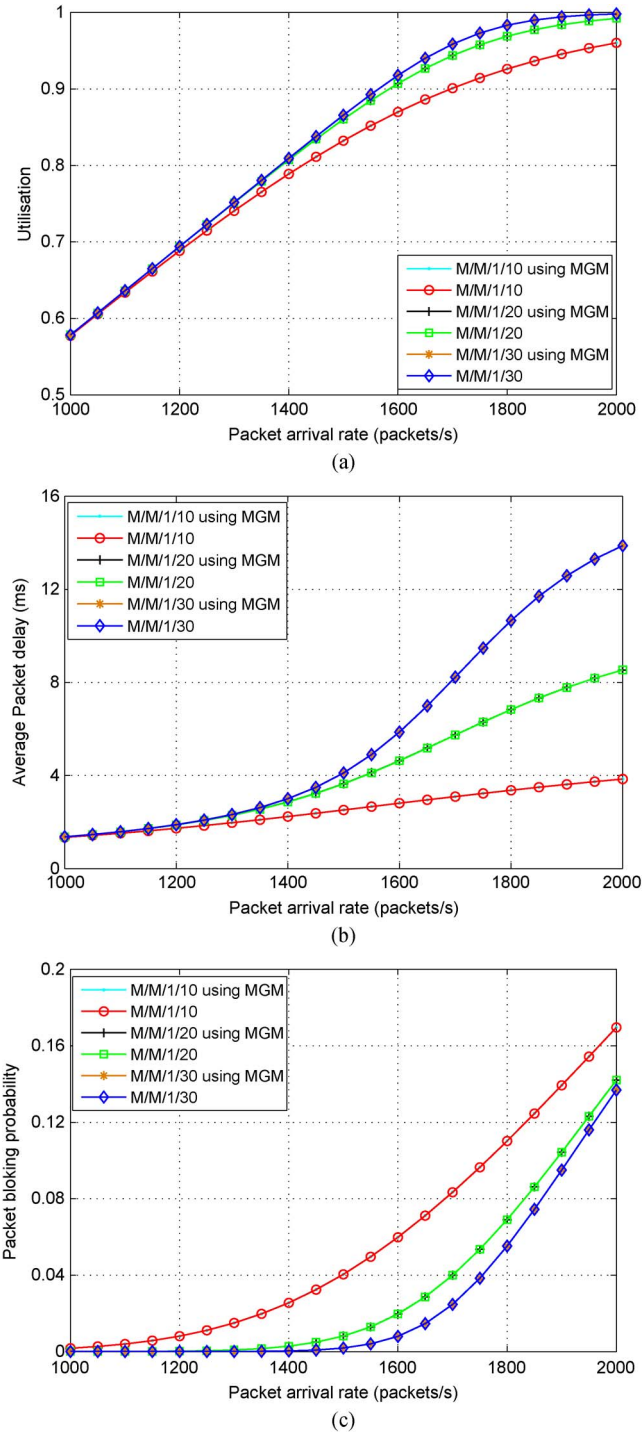

Fig. 8. Model validation. (a) Utilization. (b) Average packet delay. (c) Packet-blocking probability.

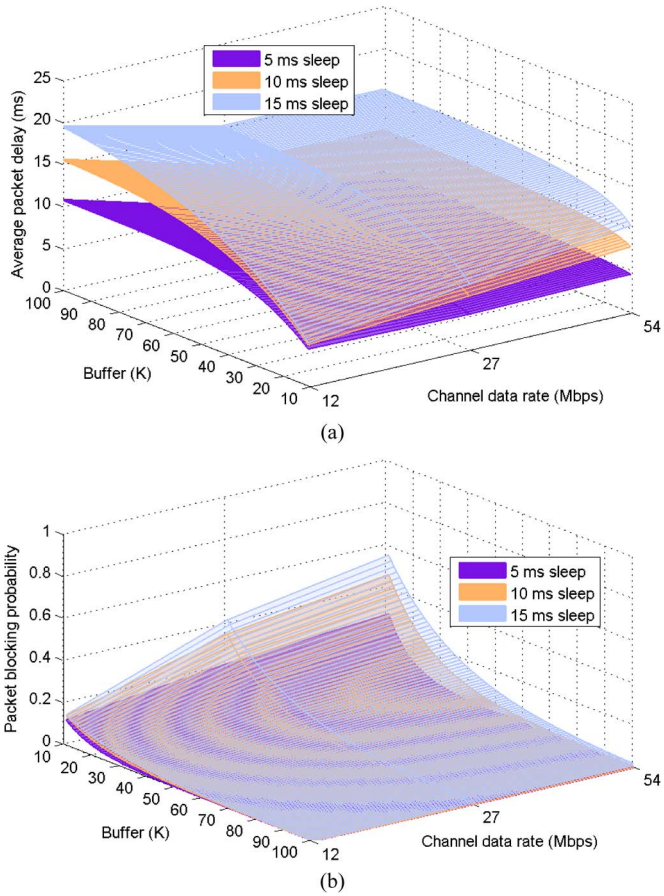

Fig. 9. Varying data rate, buffer size, and mean sleep duration. (a) Average packet delay. (b) Packet-blocking probability.

2) Varying Data Rate, Buffer Size, and Sleep Cycle on QoS Parameters: With a small buffer size, the duration of sleep cycles hardly affects the delay due to the lower number of packets waiting in the buffer, as shown in Fig. 9(a). Since the packets are served quicker at higher data rates, the AP can sleep more frequently. This results in a longer waiting time, which increases the average packet delay. As previously mentioned, the packet-blocking probability decreases with an increase in the buffer size, as shown in Fig. 9(b), although the decrement is less with a longer average sleep-cycle duration. Evidently, the longer sleep cycles incur greater packet-blocking probability because more packets will be in the buffer, waiting to be served, and consequently, further arrived packets will find the buffer full and be blocked. Thus, the proper choice of design and sleep-cycle operating parameters is crucial to maintaining the QoS (average packet delay and packet-blocking probability) thresholds. To maintain end-to-end (vehicle to main BS) QoS for video and audio conferencing applications, the average packet delay should be less than 150 and 20 ms, respectively [12]. In addition, the overall packets discarded should be less than 5%. Therefore, we choose an operating channel data rate of 27 Mb/s [41] and fix the buffer size at 64 packets for the AP.

3) Performance Evaluation: As mentioned earlier, to maintain the end-to-end QoS for packet loss and average packet delay, the packet-blocking probability and the average packet delay at the AP should be bounded at each hour of the day depending upon the achieved QoS at the M-PRMA links. Thus, the performance of the AP is analyzed in terms of average packet delay, packet-blocking probability, and the energy savings through sleep cycles. We consider three operating scenarios: 1) *bounded delay,* which is the end-to-end delay kept within the 20-ms bound while achieving maximum energy savings at each hour of the day; 2) *bounded blocking,* which is the end-to-end blocking kept within a 5% bound while

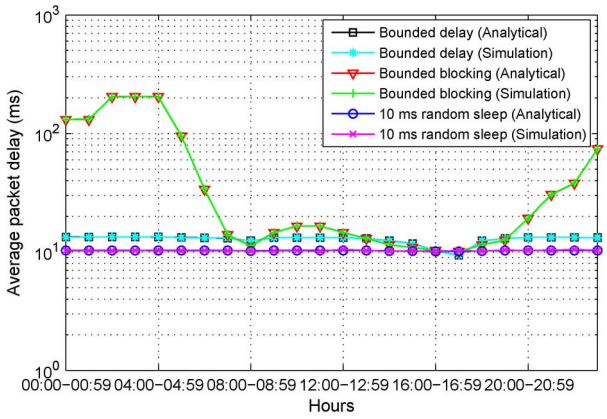

Fig. 10. Average packet delay with varying vehicular load.

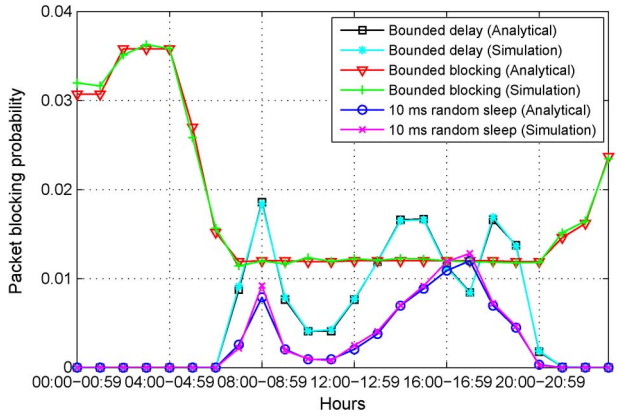

Fig. 11. Packet-blocking probability with varying vehicular load.

achieving maximum energy savings at each hour of the day; and 3) *random sleep (10 ms),* which is the random sleep cycle with mean duration of 10 ms operated at the AP to obtain energy savings at each hour of the day. Since the average packet delay at the M-PRMA links was $\leq$ 10 ms throughout the day, therefore, mean duration of 10 ms was selected in the case of a random sleep scenario. Note that the first two scenarios require traffic sensing to set the sleep-cycle duration at each hour of the day. Hence, these can be classified as reactive random sleep strategies. However, the third scenario uses proactive approach where the mean duration of sleep cycles is fixed in advance throughout the day depending upon the end-to-end QoS requirement. Thus, this can be classified as a proactive random sleep strategy. The bounded delay scenario considers end-to-end delay, which comprises the average packet delay in the M-PRMA protocol and the average packet delay at the AP. Similarly, the bounded blocking scenario considers end-to-end packet loss, which comprises of the packet-loss ratio in the M-PRMA protocol and the packet-blocking probability at the AP. The analytical results are verified through simulations for each scenario. Note that future APs should support burst-mode traffic to operate sleep cycles, similar to the chip sets provided by Broadcom for frame bursting, to improve system performance [42]. The duration of the sleep strategy can be proactive (user defined) or reactive (bounded delay and bounded blocking, in this paper). In the case of reactive sleep strategies, there is a need to develop real-time algorithms, which adjust sleep duration dynamically based on real-time vehicular traffic and data traffic measurements. However, this is beyond the scope of this paper.

a) Average packet delay: In Fig. 10, we analyze the average packet delay at the AP for varying vehicular loads at different hours of the day in all three scenarios. It is observed that the packet-blocking probability (see Fig. 11) in scenario 1 remains within its bound. In scenario 2, we observed that the average packet delay at certain (off-peak) hours increased beyond its bound. This occurs because the AP sleeps more frequently during these lean load periods. The average packet delay in scenario 3 is observed to be marginally less than that in scenario 1 in the majority of the hours of the day as the sleep cycles operate with shorter duration during those hours. We therefore conclude that the performance of scenario 3 is the best, and the performance of scenario 2 is the worst in terms of average packet delay.

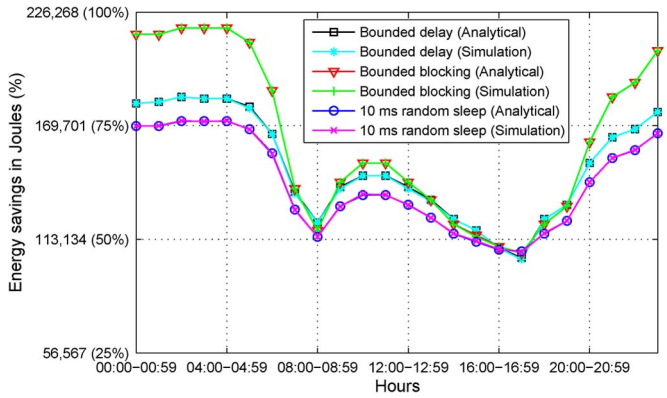

Fig. 12. Transmission energy savings with varying vehicular load.

b) Packet-blocking probability: The variation of the packet-blocking probability is shown in Fig. 11. Scenario 1 results in negligible blocking during the off-peak hours, whereas in peak hours, the blocking increases but remains within its bound. Moreover, in scenario 2, although the packet-blocking probability meets its bound at off-peak hours, the corresponding average packet delay (in Fig. 10) exceeds its bound. At peak hours of the day, the packet-blocking probability decreases well below its bound because the sleep-cycle duration is set smaller compared with the off-peak hours of the day to maintain end-to-end packet loss (due to channel impairment in M-PRMA and blocking at the AP) $\leq$ 5%. However, it is observed that scenario 3 maintains both the QoS parameters within their respective bounds. Since the respective packet-loss ratio and delay thresholds for video conferencing are 0.05 and 150 ms [40], and audio conferencing are 0.05 and 20 ms [40], the system in scenario 3 is able to support both of these applications during the whole day.

c) Energy saving: Fig. 12 shows the variation of energy savings through sleep cycles at the AP. The energy savings are shown in joules and in percentage of the transmitter energy of eight APs in the considered motorway stretch. Thus, it is not related to the operational power of the APs. In scenario 1, almost 181 kJ of energy savings (80%) was obtained at the

early hours of the day because the APs could sleep most of the time due to a very low load (i.e., number of vehicles). In contrast, they can only save 104 kJ (46%) during peak hours of the day. Note that the system design considers futuristic scenario, where the increase in number of vehicles at any hour will only result in a decrease in energy savings without affecting the QoS parameters. Overall, the trend follows the inverse of the vehicular load during the day, which is expected. In scenario 2, the maximum energy savings achieved were of 217 kJ (96%) at the early hours of the day as the APs were able to sleep most of the time, but the excess energy savings were obtained at the expense of higher average packet delay, which exceeded its threshold (see Fig. 10). A similar phenomenon occurred in the late hours of the lean load period. Although this scenario saved maximum energy throughout the day, it was not suitable from the QoS perspective. Scenario 3 only saved 170 kJ (75%) at the early hours of the day with minimum energy savings at each hour throughout the day compared with the other two scenarios. However, this scenario maintained the best QoS among all the three scenarios, and the operation did not require traffic sensing. Hence, single optimal scenario does not exist. From the system design perspective, the choice of the operating scenario and condition, therefore, depends upon the desired set of goals. Further note that, since the wake-up process of the AP incurs an energy overhead, we account that in the energy model [see (8)] as the number of sleep cycles (sleep counts), shown in Table II of Appendix C. Since no standard value of the sleep overhead was available in the literature, a reference value of 0.0175 J (see Table I) is assumed for our analysis.

D. Comparison of IEEE 802.11p and M-PRMA Protocol Performance With Sleep Cycles

Finally, we compare the performance of the IEEE 802.11p protocol with the M-PRMA protocol, as shown in Fig. 13, with the same 10-ms random sleep-cycle operation at the AP. A simplistic three-AP (node) problem is considered for ease of analysis. Since the IEEE 802.11p is a contention-based (CSMA/CA) protocol, the nodes (APs in our case) continuously sense the medium before transmission. At high load, the increased contention causes a backoff window to increase exponentially (to avoid collisions), which results in higher packet delay. In contrast, the M-PRMA ensures no contention as the nodes are aware of their respective time slots beforehand, hence reducing delay. With a simplistic assumption of uniform random transmission attempt from each of these three APs, the effective service duration in the case of IEEE 802.11p is set to three times higher than that in the case of M-PRMA protocol. The performance of both protocols has been compared in this scenario in terms of transmission energy savings [see Fig. 13(a)], average packet delay [see Fig. 13(b)], and packet-blocking probability [see Fig. 13(c)]. The M-PRMA protocol clearly outperforms the IEEE 802.11p protocol at high load, reiterating the findings shown in [11] in terms of both QoS and energy savings.

Fig. 13(a) shows energy savings, where the IEEE 802.11p clearly performs better than M-PRMA during the off-peak hours of the day. This is because it incurs lower energy overhead

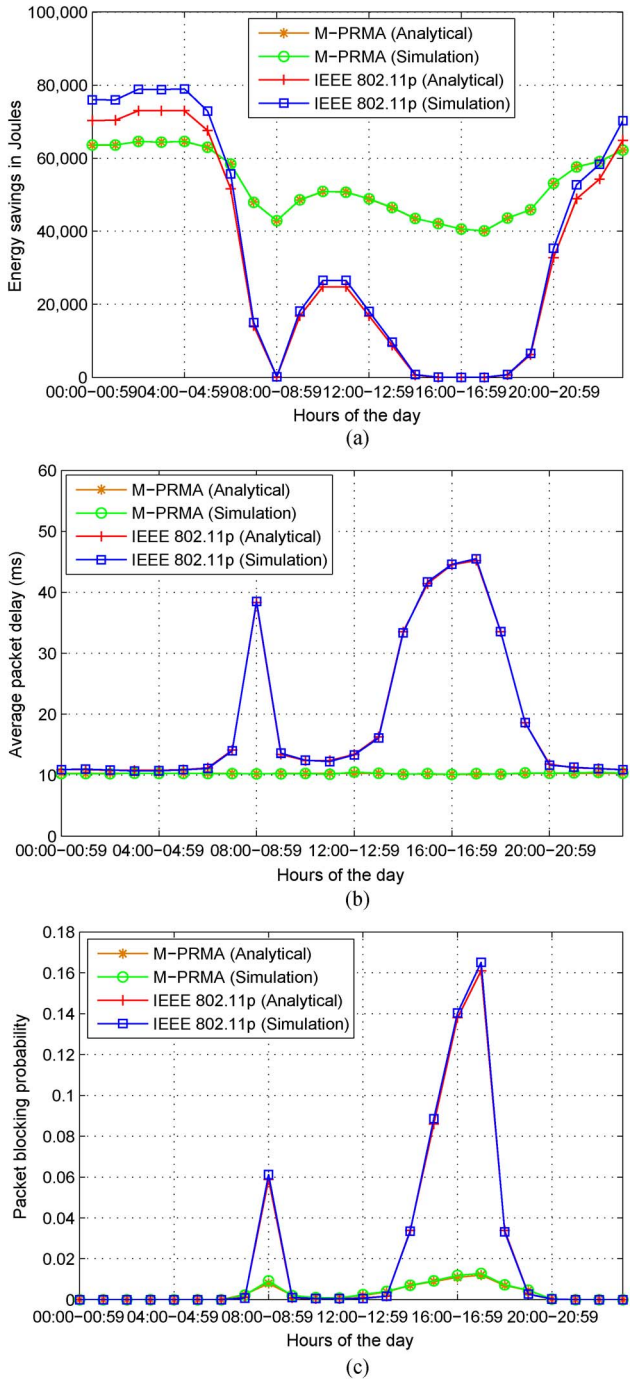

Fig. 13. Comprasion of IEEE 802.11p and M-PRMA protocols with sleep cycles in terms of (a) transmission energy savings, (b) average packet delay, and (c) Packet-blocking probability.

due to the lower sleep count as the service rate is three times lower than that of the M-PRMA protocol. However, during peak hours (07:00–20:00), the average energy savings achieved by the IEEE 802.11p is only 13% compared to 54% in the case of M-PRMA protocol. While during the whole day, the M-PRMA protocol achieved average energy savings of 62% compared to 42% in the case of IEEE 802.11p. The average packet delay in the case of IEEE 802.11p protocol reaches up to 50 ms during peak hours, which becomes unacceptable for audio conferencing application, whereas the delay remains within

a bound of 10 ms in the case of M-PRMA throughout the day. The packet-blocking probability reaches up to 17% during peak hours for the IEEE 802.11p protocol, which once again makes it unacceptable for audio conferencing applications. On the other hand, less than 1% of packet-blocking probability was observed throughout the day in the case of M-PRMA protocol.

VI. Conclusion

We have developed a vacation-based queuing analysis of a motorway vehicular communication system. Wireless channel impairments have been incorporated into the M-PRMA protocol where each time slot in outage was modeled as a server on vacation. The performance of the M-PRMA protocol with physical channel impairments has been evaluated in terms of utilization, average packet delay, and packet-loss ratio. The departure process of the M-PRMA protocol became an arrival process at the AP, which took vacations to save energy during its inactivity period. We studied the impact of three proposed operational scenarios, i.e., bounded delay, bounded blocking, and random sleep, on the system, and the performance was evaluated in terms of average packet delay, packet-blocking probability, and energy savings.

Transmission energy savings of 66%, 72%, and 62% were obtained on average in the bounded delay scenario, the bounded blocking scenario, and random sleep scenario, respectively. Both bounded delay and random sleep scenarios were able to meet the required QoS, whereas bounded blocking scenario exceeded the end-to-end delay thresholds (both audio and video conferencing) at certain hours of the day. Based on our findings in this paper, it can be concluded that each operating scenario possesses a few advantages and disadvantages. If the aim is to achieve the best QoS, regardless of maximizing energy savings, the random sleep scenario is ideal. On the other hand, if the aim is to maximize energy savings while maintaining the required QoS, the bounded delay scenario should be adopted. However, if the aim is only to maximize energy savings while sacrificing QoS at certain hours, the bounded blocking scenario should be employed.

Appendix A
Steady-State Analysis for the Number of Packets in the M-PRMA Model

Transition rate matrix Q, i.e., an infinitesimal generator, of the model shown in Fig. 2 is represented as

$$Q=\begin{bmatrix} A_0 & B & & & & & & & \\ C_1 & A_1 & B & & & & & & \\ & C_2 & A_2 & B & & & & & \\ & & \ddots & \ddots & \ddots & & & & \\ & & & C_c & A_c & B & & & \\ & & & & C & A & B & & \\ & & & & & C & A & B & \\ & & & & & & \ddots & \ddots & \ddots \end{bmatrix}. \quad (9)$$

The submatrices of Q are of dimension $(c+1)\times(c+1)$ and are given by

$$A_j=\begin{bmatrix} * & c\delta & & & & & & \\ \gamma & * & (c-1)\delta & & & & & \\ & 2\gamma & * & (c-2)\delta & & & & \\ & & \ddots & \ddots & \ddots & & & \\ & & & (c-2)\gamma & * & 2\delta & & \\ & & & & (c-1)\gamma & * & \delta & \\ & & & & & c\gamma & * & \end{bmatrix}$$

$$C_j=\begin{bmatrix} 0 & & & & & & \\ & \mu & & & & & \\ & & \ddots & & & & \\ & & & (j-1)\mu & & & \\ & & & & j\mu & & \\ & & & & & \ddots & \\ & & & & & & j\mu \end{bmatrix}.$$

$A=A_c$, $C=C_c$, and $B=\lambda I$, where I is an identity matrix of size $(c+1)\times(c+1)$. The entries not specified in the Q matrix represent the null matrices of size $(c+1)\times(c+1)$, and "$*$" in the A_j matrix represents the negative of the sum of the rates leaving that state. The entries not specified in the submatrices are zero.

The Q matrix is an infinite block tridiagonal matrix, where three blocks repeat themselves after some initial period. The proposed model follows a *quasi-birth-and-death* (QBD) process because transition from one state to the other state is not always a birth or a death, but it can be the availability/unavailability of a server from or due to a vacation. Hence, the system model can be efficiently solved using the MGM [13]. If the QBD process is ergodic and positive recurrent, then the stationary probability vector π of Q has a matrix geometric form and satisfies the following two sets of equations:

$$\pi Q=0 \quad (10)$$

$$\pi e=1 \quad (11)$$

where e is a unit column vector of the same order of π. Equation (11) states that the sum of all probabilities is unity. The stationary probability vector π may be partitioned as $(\pi_0,\pi_1,\pi_2,\ldots,\pi_{c-1},\pi_c,\ldots)$, where $\pi_k=(\pi(0,k),\pi(1,k),\pi(2,k),\ldots,\pi(c,k))$ is the probability vector of k packets in the system. By solving the set of (10), we obtain

$$\begin{aligned} \pi_0A_0+\pi_1C_1&=0\\ \pi_0B+\pi_1A_1+\pi_2C_2&=0\\ \pi_1B+\pi_2A_2+\pi_3C_3&=0\\ &\vdots\\ \pi_{c-2}B+\pi_{c-1}A_{c-1}+\pi_cC_c&=0\\ \pi_{k-1}B+\pi_kA+\pi_{k+1}C&=0,\quad k=c,c+1,\ldots \end{aligned} \quad (12)$$

It may be shown that there exists a square matrix R of order $(c+1)$, such that

$$\pi_k=\pi_{c-1}R^{k-c+1},\quad k\geqslant c. \quad (13)$$

Rewriting (12) for $k=c-1$, we obtain

$$\pi_{c-2}B+\pi_{c-1}A+\pi_cC=0. \quad (14)$$

Using (13), (14) can be written as

$$\begin{aligned}\pi_{c-2}B+\pi_{c-1}A+\pi_{c-1}RC&=0\\ \pi_{c-2}B+\pi_{c-1}(A+RC)&=0.\end{aligned}\tag{15}$$

To obtain the initial probability subvector $\pi'=(\pi_0,\pi_1,\pi_2,\ldots,\pi_{c-1})$, we define an infinitesimal generator Q' that satisfies the following system of equations:

$$\pi' Q'=0\tag{16}$$

where

$$Q'=\begin{bmatrix}A_0 & B & & & \\ C_1 & A_1 & B & & \\ & C_2 & A_2 & B & \\ & & \ddots & \ddots & \\ & & & C_{c-1} & (A_{c-1}+RC)\end{bmatrix}.\tag{17}$$

To compute R, we rewrite (12) as

$$\begin{aligned}\pi_{k-1}B+\pi_kA+\pi_{k+1}C&=0\\ \pi_{c-1}R^{(k-1)-c+1}B+\pi_{c-1}R^{k-c+1}A+\pi_{c-1}R^{(k+1)-c+1}C&=0\\ \pi_{c-1}R^{k-c}(B+RA+R^2C)&=0.\end{aligned}\tag{18}$$

Hence, R is the unique minimal nonnegative solution to the matrix quadratic equation, i.e.,

$$B+RA+R^2C=0.\tag{19}$$

Since matrix A is nonsingular, using (19), we obtain

$$R=-BA^{-1}-R^2CA^{-1}.\tag{20}$$

The spectral radius of rate matrix $\mathrm{sp}(R)$, which is the eigenvalue of R with the largest modulus, lies strictly inside the unit circle and is given by

$$\mathrm{sp}(R)<1.\tag{21}$$

Let the stationary distribution of the infinitesimal generator $A'=A+B+C$ be $\pi_{A'}$. For the QBD process to be ergodic (i.e., $\mathrm{sp}(R)<1$ and the system is stable), the following condition must hold:

$$\pi_{A'}Be<\pi_{A'}Ce.\tag{22}$$

To solve R, Neuts [13] has proposed a successive substitution procedure given by

$$R_{(0)}=0,\quad R_{(m+1)}=-V-R_{(m)}^2W\quad m=0,1,2,\ldots\tag{23}$$

where m is the index of iteration. The sequence of R_m is nondecreasing and converges to the R matrix. The iterative procedure of (23) is carried out until the maximum entrywise difference between approximations is less than a specified tolerance criterion (say 10^{-12} in our case).

Once subvectors $\pi_0,\pi_1,\pi_2,\ldots,\pi_{c-1}$ and rate matrix R are known, the remaining probability subvectors can be determined using (13). The steady-state distribution of the number of packets in the system is given as

$$p_k=\begin{cases}\pi_k e & 0\le k\le c-1\\ \pi_{c-1}R^{k-c+1}e & k\ge c.\end{cases}\tag{24}$$

Appendix B
Steady-State Analysis for the Number of Packets in AP Model

The infinitesimal generator Q matrix is of the following form:

$$Q=\begin{bmatrix}A_0 & B_0 & & & & & & \\ C_0 & A & B & & & & & \\ & C & A & B & & & & \\ & & & \ddots & \ddots & \ddots & & \\ & & & & C & A & B & \\ & & & & & C & A_1 & B_1\\ & & & & & & C_1 & A_2\end{bmatrix}\tag{25}$$

where the submatrices of Q are given by

$$\begin{aligned}A&=\begin{bmatrix}-(\lambda_s+\delta_v) & \delta_v\\ 0 & -(\lambda_s+\mu_s)\end{bmatrix}\quad B=\begin{bmatrix}\lambda_s & 0\\ 0 & \lambda_s\end{bmatrix}\\ C&=\begin{bmatrix}0 & 0\\ 0 & \mu_s\end{bmatrix}\quad A_0=-\lambda_s\quad B_0=[\,\lambda_s\quad 0\,]\\ C_0&=\begin{bmatrix}0\\ \mu_s\end{bmatrix}\quad A_1=\begin{bmatrix}-\delta_v & \delta_v\\ 0 & -(\lambda_s+\mu_s)\end{bmatrix}\\ B_1&=\begin{bmatrix}0\\ \lambda_s\end{bmatrix}\quad C_1=[\,0\quad \mu_s\,]\quad A_2=-\mu_s\end{aligned}$$

and the entries not mentioned in Q are null matrices. For the state diagram in Fig. 7, the Q is a finite block tridiagonal matrix, where three blocks repeat after initial three states (representing 0 or 1 packet), up to the states corresponding to $K-2$ packets in the system. This system follows a QBD process because transition from one state to the next state is not always a birth or a death but can be the arrival of the server from a vacation [13]. For this QBD process to be ergodic and positive recurrent, the stationary probability vector π of Q should have a matrix geometric form and must satisfy the following two systems of equations:

$$\pi Q=0\tag{26}$$

$$\pi e=1.\tag{27}$$

Following the solving procedure of (12) and (13), an explicit solution of (26) and (27) for rate matrix R and initial probabilities π_0 and π_1 (representing probabilities of 0 and 1 packet in the system), we obtain

$$\begin{aligned}R&=\begin{bmatrix}\frac{\lambda_s}{\lambda_s+\delta_v} & \frac{\lambda_s}{\mu_s}\\ & \frac{\lambda_s}{\mu_s}\end{bmatrix}\\ \pi_0&=\frac{\delta_v(\mu_s-\lambda_s)}{\mu_s(\lambda_s+\delta_v)}\\ \pi_1&=[\pi_{01}\quad \pi_{11}]=\begin{bmatrix}\dfrac{\lambda_s\delta_v(\mu_s-\lambda_s)}{\mu_s(\lambda_s+\delta_v)^2} & \dfrac{\lambda_s\delta_v(\mu_s-\lambda_s)}{\mu_s^2(\lambda_s+\delta_v)}\end{bmatrix}.\end{aligned}$$

The probability vectors of k $(2 \leq k \leq K-2)$ packets can be computed with the help of R and π_1 as

$$\pi_k = \pi_1 R^{k-1} \quad 2 \leq k \leq K-2. \tag{28}$$

To determine the probability vectors of $K-1$ and K packets, we use (26) and obtain

$$\begin{aligned} \pi_{K-1} &= -\pi_{K-2} B \left(A_1 + \frac{1}{\mu_s} B_1 C_1 \right) \\ &= -\pi_1 R^{(K-2)-1} B \left(A_1 + \frac{1}{\mu_s} B_1 C_1 \right) \end{aligned} \tag{29}$$

$$\pi_K = -\pi_{K-1} B_1 A_2^{-1}. \tag{30}$$

The steady-state distribution, describing the number of packets in the scenario, is

$$p_k = \begin{cases} \pi_k e & 1 \leq k \leq K-1 \\ \pi_k & k = 0,\ K. \end{cases} \tag{31}$$

REFERENCES

[1] *National Travel Survey: 2011, Statistical Release*, Department of Transport, London, U.K., Dec. 2012.

[2] *Vehicle Licensing Statistics, Great Britain: Quarter 3 2012*, Department for Transport, London, U.K., Dec. 2012.

[3] F. Richter, A. Fehske, and G. Fettweis, "Energy efficiency aspects of base station deployment strategies for cellular networks," in *Proc. IEEE 70th Veh. Technol. Conf.*, Sep. 2009, pp. 1–5.

[4] SMART 2020: Enabling the low carbon economy in the information age, The Climate Group, London, U.K., Tech. Rep. [Online]. Available: http://www.smart2020.org/_assets/files/02_Smart2020Report.pdf

[5] A. Capone, "Energy and mobility: Scalable solutions for the mobile data explosion," in *Proc. TIA GreenTouch Open Forum*, Jun. 2012, pp. 1–26, Politecnico di Milano.

[6] S.-E. Elayoubi, L. Saker, and T. Chahed, "Optimal control for base station sleep mode in energy efficient radio access networks," in *Proc. IEEE INFOCOM*, Apr. 2011, pp. 106–110.

[7] P. Belanovic, D. Valerio, A. Paier, T. Zemen, F. Ricciato, and C. Mecklenbrauker, "On wireless links for vehicle-to-infrastructure communications," *IEEE Trans. Veh. Technol.*, vol. 59, no. 1, pp. 269–282, Jan. 2010.

[8] T. S. Rappaport, *Wireless Communications: Principles and Practice*. Upper Saddle River, NJ, USA: Prentice-Hall, 2002.

[9] K. Bilstrup, "A survey regarding wireless communication standards intended for a high-speed vehicle environment," Halmstad Univ., Halmstad, Sweden, Tech. Rep. IDE0712, Feb. 2007.

[10] E. G. S. K. Bilstrup, E. Uhlemann, and U. Bilstrup, "On the ability of IEEE 802.11p and STDMA to provide predictable channel access," in *Proc. 16th World Congr. ITS*, Sep. 2009, pp. 5690–5699.

[11] W. Kumar, A. Muhtar, B. R. Qazi, and J. M. H. Elmirghani, "Energy and QoS evaluation for a V2R network," in *Proc. IEEE GLOBECOM*, Dec. 2011, pp. 1–5.

[12] B. R. Qazi, H. Alshaer, and J. M. H. Elmirghani, "Analysis and design of a MAC protocol and vehicular traffic simulator for multimedia communication on motorways," *IEEE Trans. Veh. Technol.*, vol. 59, no. 2, pp. 734–741, Feb. 2010.

[13] W. J. Stewart, *Probability, Markov Chains, Queues, and Simulation: The Mathematical Basis of Performance Modeling*. Princeton, NJ, USA: Princeton Univ. Press, 2009.

[14] W. Kumar, S. Bhattacharya, B. R. Qazi, and J. M. H. Elmirghani, "An energy efficient double cluster head routing scheme for motorway vehicular networks," in *Proc. IEEE ICC*, Jun. 2012, pp. 141–146.

[15] C. Fraleigh, S. Moon, B. Lyles, C. Cotton, M. Khan, D. Moll, R. Rockell, T. Seely, and S. Diot, "Packet-level traffic measurements from the Sprint IP backbone," *IEEE Netw.*, vol. 17, no. 6, pp. 6–16, Nov./Dec. 2003.

[16] M. Takai, J. Martin, and R. Bagrodia, "Effects of wireless physical layer modeling in mobile ad hoc networks," in *Proc. 2nd ACM Int. Symp. Mobile Ad Hoc Netw. Comput.*, 2001, pp. 87–94.

[17] A. Polydoros, K. Dessouky, J. Pereira, C. Sun, K. Lee, T. Papavassiliou, and V. Li, "Vehicle to roadside communications study," Univ. California, Berkeley, CA, USA, PATH Res. Rep. UCB-ITS-PRR-93-4, 1993.

[18] S. Moser, F. Kargl, and A. Keller, "Interactive realistic simulation of wireless networks," in *Proc. IEEE Symp. Interactive Ray Tracing*, Sep. 2007, pp. 161–166.

[19] J. S. Davis and J. Linnartz, "Vehicle to vehicle RF propagation measurements," in *Proc. 28th Asilomar Conf. Signals, Syst. Comput.*, 1994, vol. 1, pp. 470–474.

[20] S. Chia, "1.7 GHz propagation measurements for highway microcells," *Electron. Lett.*, vol. 26, no. 16, pp. 1279–1280, Aug. 1990.

[21] B. J. Singh, K. K. Aggrawal, and S. Kumar, "Characterization of the propagation environment by field measurements," *J. Inst. Eng. India*, vol. 88, pp. 22–25, Jul. 2010.

[22] J. Zhang, Q. Zhang, and W. Jia, "VC-MAC: A cooperative MAC protocol in vehicular networks," *IEEE Trans. Veh. Technol.*, vol. 58, no. 3, pp. 1561–1571, Mar. 2009.

[23] K. Fujimura and T. Hasegawa, "A collaborative MAC protocol for inter-vehicle and road to vehicle communications," in *Proc. 7th Int. IEEE Conf. Intell. Transp. Syst.*, Oct. 2004, pp. 816–821.

[24] K. Fujimura and T. Hasegawa, "Performance evaluation of the MAC protocol for integrated inter-vehicle and road to vehicle," in *Proc. IEEE Intell. Transp. Syst.*, Sep. 2005, pp. 308–313.

[25] T. Zhou, H. Sharif, M. Hempel, P. Mahasukhon, W. Wang, and T. Ma, "A novel adaptive distributed cooperative relaying MAC protocol for vehicular networks," *IEEE J. Sel. Areas Commun.*, vol. 29, no. 1, pp. 72–82, Jan. 2011.

[26] S. Chen, A. Wyglinski, R. Vuyyuru, and O. Altintas, "Feasibility analysis of vehicular dynamic spectrum access via queueing theory model," in *Proc. IEEE VNC*, Dec. 2010, pp. 223–230.

[27] B. Vinod, "Exponential queues with server vacations," *J. Oper. Res. Soc.*, vol. 37, no. 10, pp. 1007–1014, Oct. 1986.

[28] P. Kolios, V. Friderikos, and K. Papadaki, "Ultra lower energy store-carry and forward relaying within the cell," in *Proc. IEEE 70th VTC-Fall*, Sep. 2009, pp. 1–5.

[29] E. Callaway, "Low power consumption features of the IEEE 802.15.4/Zigbee LRWPAN standard," in *Proc. Mini-Tutorial, ACM Sensys*, Los Angeles, CA, USA, Nov. 2003, pp. 1–40.

[30] C.-S. Hsu and Y.-C. Tseng, "Cluster-based semi-asynchronous power-saving protocols for multi-hop ad hoc networks," in *Proc. IEEE ICC*, May 2005, pp. 3166–3170.

[31] L. Ning, X. Yuan, and X. Sheng-li, "A power-saving protocol for ad hoc networks," in *Proc. Int. Conf. Wireless Commun., Netw. Mobile Comput.*, Sep. 2005, vol. 2, pp. 808–811.

[32] L. Haratcherev, M. Fiorito, and C. Balageas, "Low-power sleep mode and out-of-band wake-up for indoor access points," in *Proc. IEEE GLOBECOM Workshops*, Nov./Dec. 2009, pp. 1–6.

[33] W. Fisher, M. Suchara, and J. Rexford, "Greening backbone networks: reducing energy consumption by shutting off cables in bundled links," in *Proc. 1st ACM SIGCOMM Workshop Green Netw.*, New York, NY, USA, 2010, pp. 29–34.

[34] M. Gupta and S. Singh, "Greening of the Internet," in *Proc. SIGCOMM Conf. Appl., Technol., Architect., Protocols Comput. Commun.*, New York, NY, USA, 2003, pp. 19–26.

[35] S. Zhou, J. Gong, Z. Yang, Z. Niu, and P. Yang, "Green mobile access network with dynamic base station energy saving," presented at the ACM MobiCom, Beijing, China, Sep. 20–25, 2009, Paper 31.

[36] G. Narlikar, S. Bhaumik, S. Chattopadhyay, and S. Kanugovi, "Green, energy-efficient network re-organization," Alcatel-Lucent India, Bangalore, India, Tech. Rep., 2011.

[37] S.-H. Wu, C.-M. Chen, and M.-S. Chen, "An asymmetric and asynchronous energy conservation protocol for vehicular networks," *IEEE Trans. Mobile Comput.*, vol. 9, no. 1, pp. 98–111, Jan. 2010.

[38] *IEEE P802.11p/D7.0, Draft for Wireless Access in Vehicular Environments (WAVE)*, IEEE Std. P802.11p/D7.0, May 2009.

[39] A. Goldsmith, *Wireless Communications*. Cambridge, U.K.: Cambridge Univ. Press, 2005.

[40] X. Wu, S. Wu, H. Sun, and L. Li, "Dynamic slot allocation multiple access protocol for wireless ATM networks," in *Proc. IEEE ICC*, Jun. 1997, vol. 3, pp. 1560–1565.

[41] Smarter vehicles, safer roads MCNU R1551, Kapsch, Vienna, Austria, Tech. Rep. [Online]. Available: http://ww1.prweb.com/prfiles/2008/10/22/915544/MCNUR1551.PDF

[42] Broadcom Corporation, Irvine, CA, USA. [Online]. Available: http://www.broadcom.com/products/Wireless-LAN

Wanod Kumar received the B.Eng. degree from Mehran University of Engineering and Technology, Jamshoro, Pakistan, and the M.Sc. and Ph.D. degrees in electronic and electrical engineering from the University of Leeds, Leeds, U.K.

He is currently an Assistant Professor with the Department of Electronic Engineering, Mehran University of Engineering and Technology. His research interests include energy-efficient wireless networks, particularly vehicular networks, and medium access control and routing protocols.

Samya Bhattacharya (M'13) received the B.E. degree in electrical engineering from Jadavpur University, Kolkata, India, in 2000; the M.Tech. degree in computer science and engineering from Vellore Institute of Technology, Vellore, India, in 2002; and the Ph.D. degree in electrical engineering from the Indian Institute of Technology Delhi, New Delhi, India, in 2008.

From July 2002 to December 2002, he was a Project Trainee with the Advanced Computing and Microelectronics Unit, Indian Statistical Institute, Kolkata. From April 2008 to August 2010, he was a research scientist with the Innovation Labs, Tata Consultancy Services Limited: Performance Engineering, Mumbai, India, and Kolkata, India. He is currently a Research Fellow and a Project Manager with the School of Electronic and Electrical Engineering, University of Leeds, U.K. His current research interests include performance- and energy-efficient traffic engineering, stochastic modeling, network calculus, call admission control, and quality of service in next-generation communication systems.

Dr. Bhattacharya is a life member of Institution of Communication Engineers and Information Technologists, India. He has served as a member of the Technical Program Committee for the IEEE Sarnoff Symposium, the IEEE International Conference on Communications (2010–2014), the IEEE Global Communications Conference (2010–2014), the IEEE International Conference on Industrial Technology Workshop, and a number of conferences organized by the IEEE Communication Society.

Bilal R. Qazi (M'10) received the B.Sc. degree in computer science from the University of the Punjab, Lahore, Pakistan, in 2001; the M.Phil. degree in electrical engineering from Swansea University, Swansea, U.K., in 2004; and the Ph.D. degree, also in electrical engineering, from the University of Leeds, Leeds, U.K.

During his studies, he worked as a Part-Time Research Assistant with the School of Electronic and Electrical Engineering, University of Leeds. Since June 2010, he has been a Postdoctoral Research Fellow with the University of Leeds. His research interests include vehicular networks, multimedia communications, medium-access-control and routing protocols, energy efficiency, and quality-of-service provisioning.

Dr. Qazi is a member of Oracle and Sun Microsystems. He has been a member of the Technical Program Committee for the IEEE Global Communications Conference and the IEEE International Conference on Communications since 2010.

Jaafar M. H. Elmirghani (SM'08) received the B.Sc. degree (First-Class Hons.) in electrical engineering from the University of Khartoum, Khartoum, Sudan, in 1989 and the Ph.D. degree from the University of Huddersfield, West Yorkshire, U.K., in 1994, for work on optical receiver design and synchronization.

From 2000 to 2007, he was a Professor with Swansea University (formerly known as University of Wales Swansea), Swansea, U.K. Since 2007, he has been with the University of Leeds, Leeds, U.K., where he is currently the Director of the Institute of Integrated Information Systems and a Professor of communication networks and systems with the School of Electronic and Electrical Engineering. He is the author of over 375 technical papers and a Co-Editor of *Photonic Switching Technology: Systems and Networks* (IEEE Press, 1998). He also leads a number of research projects. His research interests include communication networks, wireless and optical communication systems.

Dr. Elmirgani is a Fellow of the Institution of Engineering and Technology (IET) and a Fellow of the Institute of Physics. He was a member of the Technical Activities Council and the Chair of the Transmission Access and Optical Systems Committee and the Signal Processing and Communication Electronics Committee of the IEEE Communication Society. He served as the Chair for the IEEE U.K. and Republic of Ireland Communications Chapter. He has been on the Technical Program Committee of 31 IEEE Global Communications Conferences (IEEE GLOBECOM)/IEEE International Conferences on Communications (IEEE ICC) between 1995 and 2013, where he served 13 times as a Symposium Chair/Track Chair. He was the Founding Chair of the Advanced Signal Processing for Communication Symposium, which started at the IEEE GLOBECOM in 1999 and has continued since at every IEEE ICC and GLOBECOM. He was also the founding Chair of the first IEEE ICC/GLOBECOM Optical Symposium at the IEEE GLOBECOM in 2000. He has served as the Chair for the Future Photonic Network Technologies, Architectures, and Protocols Symposium. He is the Chair of the IEEE Green ICT Committee within the IEEE Technical Activities Board Future Directions Committee, which is an IEEE Societies committee responsible for Green ICT activities in IEEE (2012–2015). He is the founding Chair of the 2011 IEEE GLOBECOM Selected Areas in Communications, Green Communication Systems, and Networks Track. The track has taken place at the IEEE GLOBECOM in 2012 and the IEEE ICC in 2013 and will take place at the IEEE ICC in 2014. He is a Co-Chair of the GreenTouch Core Switching and Routing Working Group, an Adviser to the Commonwealth Scholarship Commission, a member of the Royal Society International Joint Projects Panel, and a member of the Engineering and Physical Sciences Research Council (EPSRC) College. He is a Distinguished Lecturer of IEEE Communication Society for 2013–2014. He served as an Editor for IEEE COMMUNICATIONS MAGAZINE. He is currently serving as an Editor for *IET Optoelectronics* and the *Journal of Optical Communications.* He received the IEEE Communications Society Hal Sobol Award for exemplary service to meetings and conferences and the IEEE Communications Society Chapter Achievement Award in 2005, the University of Wales Swansea inaugural Outstanding Research Achievement Award in 2006, the IEEE Communications Society Signal Processing and Communication Electronics Outstanding Service Award in 2009, and the IEEE ICC Best Paper Award in 2013. He has been awarded in excess of £20 million in grants to date from the Environmental and Physical Sciences Research Council of the U.K., the European Union, and industries and has held prestigious fellowships funded by the Royal Society and by BT.